Am J Cancer Res 2017;7(10):2051-2069
www.ajcr.us /ISSN:2156-6976/ajcr0065464

Original Article

MiR-216b functions as a tumor suppressor by targeting HMGB1-mediated JAK2/STAT3 signaling way in colorectal cancer

Xiaoxiang Chen[1,2], Xiangxiang Liu[2], Bangshun He[2], Yuqin Pan[2], Huiling Sun[2], Tao Xu[2], Xiuxiu Hu[2], Shukui Wang[1,2]

[1]Medical college, Southeast University, Nanjing 210009, Jiangsu, China; [2]General Clinical Research Center, Nanjing First Hospital, Nanjing Medical University, Nanjing 210006, Jiangsu, China

Received September 12, 2017; Accepted September 25, 2017; Epub October 1, 2017; Published October 15, 2017

Abstract: MiR-216b is implicated in the development of multiple types of cancers, however, a role for miR-216b in colorectal cancer (CRC) remains elusive. The present study aimed to investigate the function and underlying mechanism of miR-216b in human CRC. In this study, we found miR-216b in CRC tissues and cell lines was markedly decreased compared with corresponding adjacent normal tissues (ANTs) and colonic mucosal epithelial cell line (FHC), and was obviously associated with the TNM stage, lymph node metastases, differentiation and poor overall survival (OS) (P<0.05). Furthermore, we demonstrated that miR-216b inhibited cell proliferation, migration, invasion and angiogenesis by targeting HMGB1 which was highly expressed in CRC. Additionally, we proved that miR-216b promoted the development and progression of CRC, at least partially through HMGB1-mediated JAK2/STAT3 pathway. Lastly, we showed that plasma miR-216b expression was reduced in CRC when compared to healthy controls and might be a potential diagnostic biomarker for CRC. The findings indicated that miR-216b might function as a suppressor in CRC and could serve as a promising diagnostic and prognostic biomarker for CRC.

Keywords: MiR-216b, colorectal cancer (CRC), HMGB1, JAK2/STAT3

Introduction

Colorectal cancer (CRC) is the third most common cancer, which accounts for approximately 10% of all cancer cases with more than 1 million new cases diagnosed worldwide annually [1]. Surgery is the main treatment for colorectal cancer and chemotherapy and molecular targeted therapy is supplementary treatments [2, 3]. Accumulating evidence showed that approximate 90% of the CRC patients who detected at an early stage could be cured by surgery, unfortunately, most patients are diagnosed at an advanced stage, leading to a poor prognosis [4]. Therefore, to find a new diagnostic and prognostic markers are in urgent demand.

MicroRNAs (MiRs) are a group of a small noncoding RNAs which interact with their target gene mRNAs by binding to the 3'-untranslated regions (UTRs). Many miRNAs have been reported to regulate a variety of biological process, such as proliferation, differentiation, migration and apoptosis [5-7]. Moreover, emerging evidences indicate that miRNAs are promising biomarkers for cancer diagnosis and prognosis [8, 9].

miR-216b is located at chromosome 2p16.1, having been reported to act as a tumor suppressor in many cancers. Min Deng *et al.* reported that miR-216b is downregulated and inhibit tumor growth and invasion by targeting KRAS in nasopharyngeal carcinoma (NPC) [10]. Our previous study have shown that miR-216b is low expression and suppresses cell proliferation, colony formation, cell migration and induce cycle arrest in HCC cells [11].

High mobility group box 1 (HMGB1) is a 25 to 30 kDa protein, belonging to HMGB family members, which has been reported to act as an extracellular signaling molecule in a diversity of biological processes, including inflammation,

Table 1. Correlation between miR-216b expression and different clinical characteristics

Characteristics	No. of Patients (%) (n=84)	MiR-216b expression		*p* value
		Low (%) (n=42)	High (%) (n=42)	
Age (years)				0.500
<60	31 (36.9%)	17 (40.5%)	14 (33.3%)	
≥60	53 (63.1%)	25 (59.5%)	28 (66.7%)	
Sex				0.278
Female	41 (49.4%)	18 (42.9%)	23 (54.8%)	
Male	43 (50.6%)	24 (57.1%)	19 (45.2%)	
Tumor location				0.828
Colon	45 (53.6%)	23 (54.8%)	22 (52.4%)	
Rectum	39 (46.4%)	19 (45.2%)	20 (47.6%)	
Tumor size (cm)				0.327
<5	33 (39.3%)	15 (35.8%)	18 (42.9%)	
≥5	51 (60.7%)	27 (64.2%)	24 (57.1%)	
Differentiation				<0.01
Well	8 (9.5%)	4 (9.5%)	4 (9.5%)	
Moderate	53 (63.1%)	20 (47.6%)	33 (78.6%)	
Poor	23 (27.4%)	18 (42.9%)	5 (11.9%)	
Serum CEA level (ng/mL)				0.509
<10	35 (41.7%)	19 (45.2%)	16 (38.1%)	
≥10	49 (58.3%)	23 (54.8%)	26 (61.9%)	
Local invasion				0.581
T1-T2	16 (19.0%)	7 (16.7%)	9 (19.0%)	
T3-T4	68 (81.0%)	35 (83.3%)	33 (81.0%)	
Lymph node metastasis				0.014
N0	46 (54.8%)	21 (50.0%)	25 (59.5%)	
N1	27 (32.1%)	11 (26.2%)	16 (38.1%)	
N2	11 (13.1%)	10 (23.8%)	1 (2.4%)	
TNM stage				<0.01
I	6 (7.1%)	1 (15.4%)	5 (2.2%)	
II	38 (45.2%)	11 (46.2%)	27 (44.4%)	
III	40 (47.7%)	30 (38.4%)	10 (53.4%)	

cell migration and tumor metastasis [12, 13]. Mounting evidence has shown that HMGB1 plays a critical role in many kinds of cancers, including breast cancer, lung cancer, gastric cancer and colorectal cancer [14-17]. Yao X *et al.* reported that overexpression of HMGB1 is associated with poor overall survival in patients with CRC [18].

In our study, we aimed to explore the role of miR-216b on development and progression of CRC and its value of prognosis and diagnosis in CRC.

Materials and methods

Patients and participants

Colorectal cancer and matched adjacent normal tissues (ANTs) were obtained from 84 CRC patients who underwent primary surgery resection at Nanjing First Hospital with written consent. All tissue specimens were immediately stored in liquid nitrogen after surgery and stored in -80°C until RNA extraction, moreover, all these tissue specimens were also made into Paraffin sections (4 μm in thickness) stored at pathological department. Plasma samples were collected from these CRC patients and 60 healthy volunteers. Blood were collected in ethylene diamine tetraacetic acid (EDTA) anticoagulation tubes and centrifuged at 3000 g for 5 minutes. The plasma was separated into a 1.5 mL RNase-free centrifuge tube (Axygen, Union, Calif) and stored at -80°C until RNA isolation. This study was also approved by the ethics committees of Nanjing First Hospital. None of patients in this study underwent chemotherapy or radiation therapy before radical surgical resection. All clinicopathologic features of these patients were listed in **Table 1**.

Cell culture

Colonic mucosal epithelial cell line (FHC) and CRC cell lines (HCT116, HCT8 and HT29) were obtained from the Chinese Academy Medical Science (China), Cell lines were cultured in Dulbecco's modified Eagle medium (DMEM, HyClone, USA) containing 10% fetal bovine serum (FBS, HyClone, USA) in a humidified incubator under 5% CO_2 at 37°C.

Cell transfection

The miR-216b mimic, mimic negative control (NC), pcDNA3.1-HMGB1 and blank vector were purchased from Applied Biologic Materials, Inc (Canada). The corresponding sequences were as follows: miR-216b mimic: sense: 5'-AAAUCUCUGCAGGCAAAUGUGA-3' antisense: 5'-ACAUUUGCCUCCAGAGAUUUUU-3'; and mimic NC: sense: 5'-UUCUCCGAACGUGUCACGUTT-3' antisense: ACGUGACACGUUCGGAGAATT-3'; After HCT116 and HT29 cells (5×10^5 cells/well) were cultured in 6-well plates for 24 h, miR-216b-mimic, pcDNA3.1-HMGB1 or corresponding controls were transfected into HCT116 and HT29 cells by Lipofectamine 2000 reagent (Invitrogen, USA) in accordance with manufacturer's protocol, respectively.

Bioinformatics methods

The potential target genes of miR-216b were predicted using miRanda (http://www.microrna.org/) and Starbase(http://starbase.sysu.edu.cn/).

Plasmid constructs and luciferase reporter assay

The wild-type (WT) and mutant (MT) HMGB1 3'-untranslated regions (UTRs) were amplified by PCR and cloned into the pMIR-Report Luciferase vector (Ambion, USA). For luciferase assay, HT29 cells were seeded in 24 well plates, and transfected with WT or MT HMGB1 plasmid along with miR-216b mimic or miR-NC, respectively. Transfection was carried out using Lipofectamine 2000 in accordance with the manufacturer's procedure (Invitrogen, USA). Luciferase activities were analyzed 48 h after transfection using a Dual-luciferase Reporter Assay system (Promega, USA) and renilla luciferase was used for normalization.

RNA extraction and quantitative real-time PCR (qRT-PCR)

Total RNA from tissue, cell and plasma samples using TRIzol reagent (Invitrogen, USA) and miRcute Serum/plasma miRNA isolation kit (TIANGEN, China) in accordance with the manufacturers' instructions. miRNA cDNAs Synthesis Kit (Applied Biologic Materials, Inc, Canada) was performed to synthesize cDNA by reverse transcription reaction. EvaGreen miRNA qRNA MasteMix kits (Applied Biologic Materials, Inc, Canada) was performed to detect the expression of miR-216b. U6 was used as internal control for tissue samples and cells, and caenorhabditis elegans miR-39 (cel-miR-39) was used as internal control for plasma samples. For mRNA, the cDNA were reverse transcribed from total RNA using PrimeScript RT-PCR Kit (Takara, Dalian, China). RT-PCR for detecting HMGB1 mRNA expression levels in tissues and cells were performed with HMGB1 specific primes using SYBR Premix Ex TagTM II (Takara, Dalian, China) by ABI 7500 System (Applied Biosystem, Foster city, CA, USA), β-actin was used as internal control. The relative expression was calculated using $2^{-\Delta\Delta CT}$.

Western blot

Cells were harvested and lysed after 48 h transfection. Protein were separated by 10% SDS-PAGE, transferred to PVDF membranes (Millipore, USA). The membranes were blocked with Tris buffered saline with Tween 20 (TBST) containing 5% non-fat milk overnight at 4°C, then were blotted with primary antibodies against HMGB1, Janus kinase 2 (JAK2), phosphorylated JAK2 (p-JAK2, Tyr1007/1008), signal transducer and activator of transcription 3 (STAT3), phosphorylated STAT3 (p-STAT3, Try705) and β-actin (Cell Signaling Technology, USA) at a concentration of 1:1000 at 4°C overnight. After being washed, the membranes were incubated with secondary antibodies at room temperature for 1 h. Signal detection was carried out with the enhanced chemiluminescence system (ECL) reagent (KeyGEN BioTECH, China).

Immunohistochemistry

Paraffin sections from pathological department were deparaffinised in xylene, followed by rehydration in graduated alcohol, and incubated with 3% hydrogen peroxide for 10 min to block endogenous peroxidase. Epitope retrieval was performed by microwaving the slides in 0.01 M citrate buffer (pH 6.0). The sections were incubated with 10% normal goat serum for 15min at room temperature. Thereafter, the slides were incubated with anti-HMGB1 (1:500, Cell Signaling Technology, USA) overnight at 4°C and then washed with TBST (3×10 min) before incubation with secondary antibody (Dako Cytomation) for 30 min at room temperature.

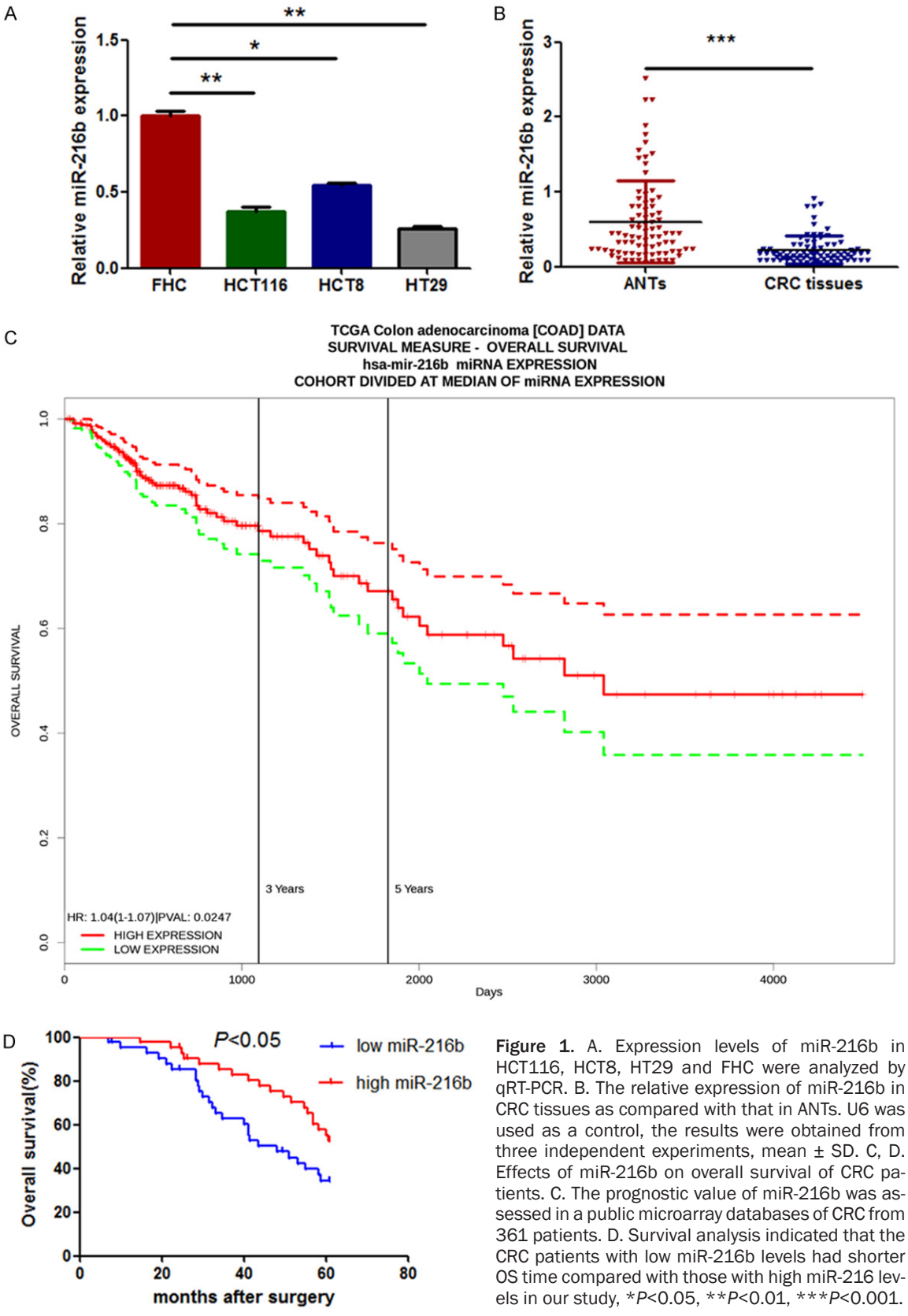

Figure 1. A. Expression levels of miR-216b in HCT116, HCT8, HT29 and FHC were analyzed by qRT-PCR. B. The relative expression of miR-216b in CRC tissues as compared with that in ANTs. U6 was used as a control, the results were obtained from three independent experiments, mean ± SD. C, D. Effects of miR-216b on overall survival of CRC patients. C. The prognostic value of miR-216b was assessed in a public microarray databases of CRC from 361 patients. D. Survival analysis indicated that the CRC patients with low miR-216b levels had shorter OS time compared with those with high miR-216 levels in our study, **P*<0.05, ***P*<0.01, ****P*<0.001.

Table 2. univariate and multivariate analysis for OS in patients with CRC

Characteristics	Multivariate analysis for OS		Univariate analysis for OS	
	HR (95% CI)	*p*	HR (95% CI)	*p*
Age (<60/≥60)	-	-	1.107 (0.705-1.739)	0.651
Gender (Female/Male)	-	-	0.851 (0.543-1.333)	0.481
Tumor location (colon/rectum)	-	-	0.808 (0.515-1.268)	0.353
Tumor size (<5/≥5)	-	-	0.923 (0.678-1.529)	0.134
Differentiation (well/moderate/poor)	1.938 (1.200-3.132)	0.017	3.848 (2.520-5.879)	0.012
CEA (<10/≥10)	-	-	0.954 (0.607-1.501)	0.840
Location invasion (T1+T2/T3+T4)	-	-	0.966 (0.496-1.883)	0.616
Lymph node metastasis (N0/N1/N2)	2.216 (1.557-3.153)	0.011	3.611 (2.506-4.604)	0.008
TNM stage (I/II/II)	1.742 (0.965-3.145)	0.01	3.506 (2.331-5.275)	<0.001
miR-216b (low/high)	0.479 (0.245-0.939)	0.032	0.257 (0.156-0.424)	0.002

For visualization, slides were incubated in the 3,3'-diaminobenzedine solution until desired staining was approached. Finally, the sections were stained by hematoxylin and observed under a microscope and images were taken by a digital camera. The intensity of staining was scored by two independent pathologist in the following four categories: no staining =0, weak staining =1, moderate staining =2 and strong staining =3. Tumor cells in 4-8 fields were selected at random, and scored based on the percentage of positively stained cells (0-100%). The finally ICH score was calculated by multiplying the percentage of positive cells with the intensity score.

Cell proliferation assay

Cells at a concentration of 5×10^3 per well were seeded in the 96-well plate and incubated for 12 h, 24 h, 48 h and 72 h. Cell viability was measured with a Cell Counting Kit-8 (CCK-8) KeyGEN BioTECH, China), following the manufacturer's instructions. The absorbance (450 nm) was assessed on a microplate reader (Bio-Tek Instruments Inc., Winooski, VT, USA).

Wound-healing assay

Wound-healing assay was used to evaluate cell migration activity. Cells were wounded by scraping of four parallel lines with a 200 μl pipette tip, then washed with PBS and incubated in serum-free DMEM. Theses wounds were photographed at 0 h and 48 h after wounding under a microscope (Olympus, Japan).

Cell invasion assay

Cell invasion assay was performed using the 24-well transwell chambers, pre-coating with Matrigel (BD Biosciences, USA). 100 μl serum-free medium, containing 2×10^5 cells, were added into upper chamber. Then, 500 μl DMEM containing 15% FBS were added into the lower chamber. The cells were fixed with Methanol and stained by 0.05% crystal violet, then counted under an inverted microscope (Olympus, Japan).

Tube formation assays

HVVECs cells (7×10^5) were suspended by the mixture of tumor-conditioned medium (TCM, 300 μl) and DMEM containing 10% FBS (300 μl), and then plated into a 24-well plate pre-coated with matrigel (200 μl per well, BD Biosciences, USA). tube formation was observed after 6 h incubation at 37°C and was imaged with a computer-assisted inverted microscope (Olympus, Japan), the number of tube branches was counted by image J software.

Statistical analysis

All experiments were performed in triplicate. The data are expressed as mean ± SD, and analyzed by SPSS 22.0 software. The Student's t-test, one-way analysis of variance (ANOVA) were used to estimated the differences between groups. Pearson's Mann-Whitney U test or χ^2 test was performed to analyze the relationship between expression of miR-216b and clinicopathological features. Kaplan-Meier method was applied to assess overall survival (OS). The survival curves were compared with log-rank test. Follow-up time was censored if the patient was lost to follow-up. Cox proportional hazards model was used to perform multivariate analysis and calculate the 95% confi-

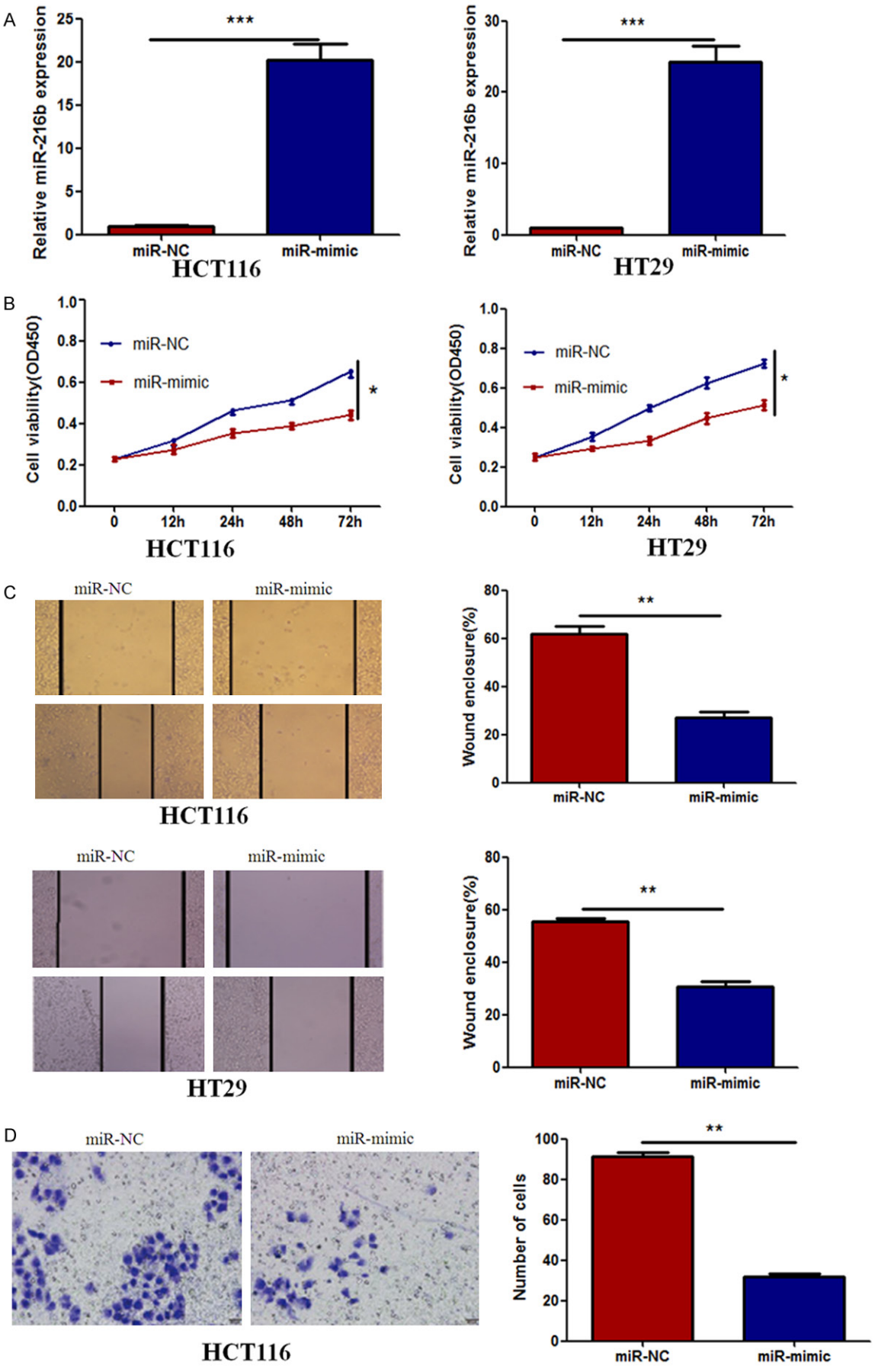
A
Relative miR-216b expression
***
miR-NC
miR-mimic
HCT116
Relative miR-216b expression
***
miR-NC
miR-mimic
HT29
B
Cell viability(OD450)
miR-NC
miR-mimic
*
0
12h
24h
48h
72h
HCT116
Cell viability(OD450)
miR-NC
miR-mimic
*
0
12h
24h
48h
72h
HT29
C
miR-NC
miR-mimic
HCT116
Wound enclosure(%)
**
miR-NC
miR-mimic
miR-NC
miR-mimic
HT29
Wound enclosure(%)
**
miR-NC
miR-mimic
D
miR-NC
miR-mimic
HCT116
Number of cells
**
miR-NC
miR-mimic

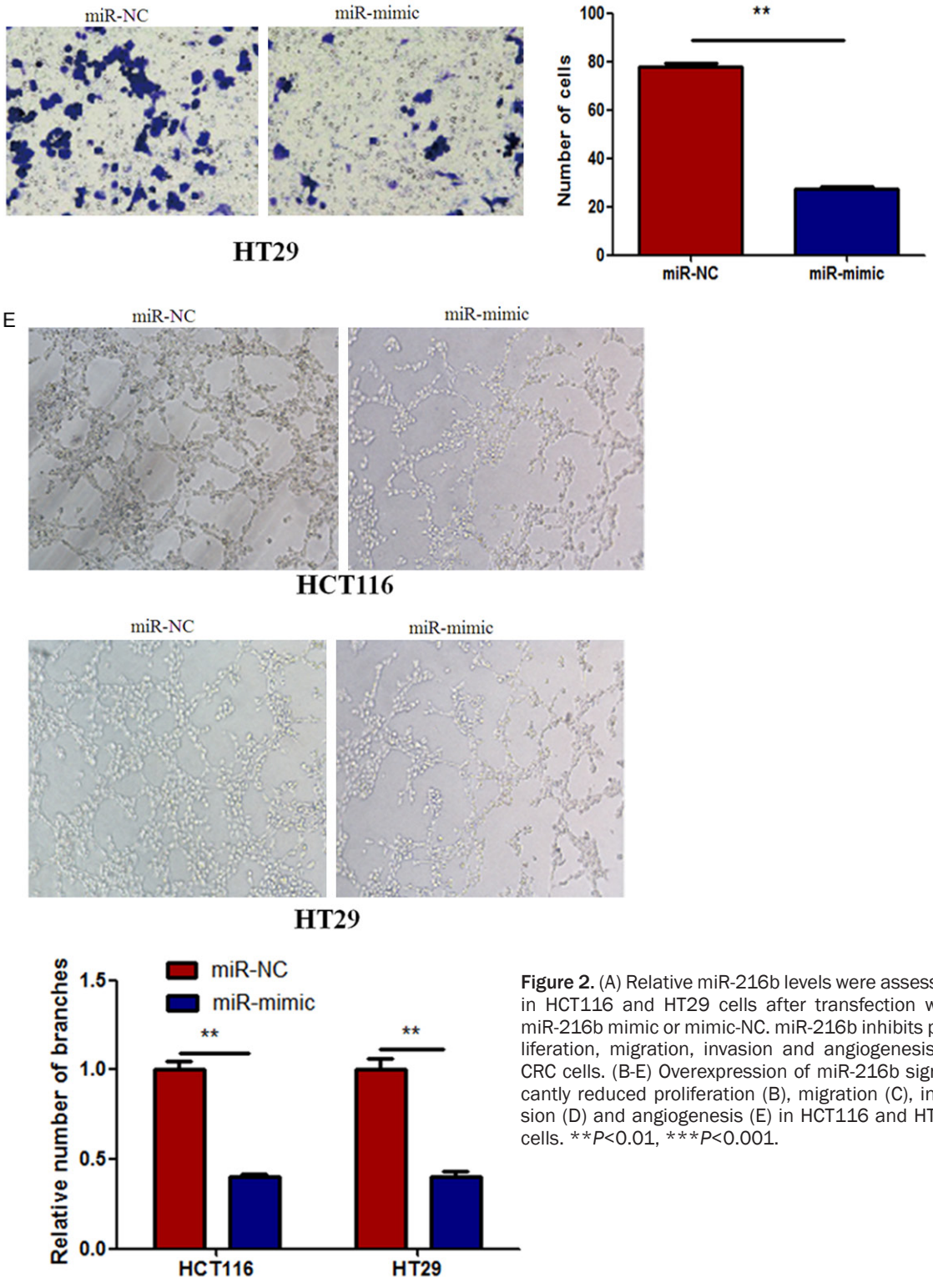

Figure 2. (A) Relative miR-216b levels were assessed in HCT116 and HT29 cells after transfection with miR-216b mimic or mimic-NC. miR-216b inhibits proliferation, migration, invasion and angiogenesis in CRC cells. (B-E) Overexpression of miR-216b significantly reduced proliferation (B), migration (C), invasion (D) and angiogenesis (E) in HCT116 and HT29 cells. $^{**}P<0.01$, $^{***}P<0.001$.

dence interval (95% CI). The area under the receiver operating characteristic (ROC) curve was performed to assess the feasibility of plasma miR-216b as a potential diagnostic biomarker for CRC. $P<0.05$ was considered to be statistically significant.

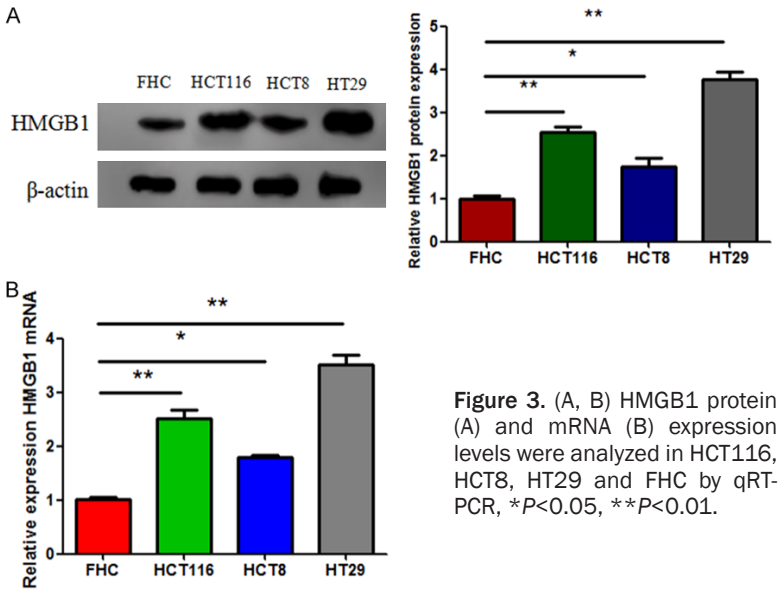

Figure 3. (A, B) HMGB1 protein (A) and mRNA (B) expression levels were analyzed in HCT116, HCT8, HT29 and FHC by qRT-PCR, **P*<0.05, ***P*<0.01.

Results

The expression of miR-216b is downregulated in CRC tissues

To evaluate the expression of miR-216b in CRC cell lines, qRT-PCR was performed in HCT116, HCT8, HT29 and FHC. We found miR-216b was significantly downregulated in CRC cell lines compared with FHC (**Figure 1A**). To confirm the association between miR-216b and CRC, we detected the expression of miR-216b in 84 paired CRC and adjacent normal tissues. Compared with ANTs, the tumor tissues exhibited generally lower miR-216b levels (**Figure 1B**).

Low expression of miR-216b in CRC tissues is associated with poor clinicopathological features and prognosis in CRC

To evaluate the clinical significance of miR-216b expression in CRC tissues, we divided the 84 CRC patients in our study into two groups (high and low miR-216b expression) with the median miR-216b expression levels serving as the cutoff point between the two groups. As shown in **Table 1**, lower levels of miR-216b was significantly correlated with differentiation, Lymph node metastasis and TNM stage (*P*< 0.05). Taken together, these findings indicated that downregulated miR-216b expression was correlated with the development and progression of CRC.

Kaplan-Meier survival analysis was then used to evaluate the relationship between the expression of miR-216b and survival time. Firstly, we examined the effect of miR-216b on overall survival (OS) in patients with CRC using online KMPLOT site, PROG gene V2. CRC patients were divided into two subgroups, high miR-216b and low miR-216b, based on their median expression. As shown in **Figure 1C**, compared with patients with a high miR-216b expression, the patients with a low miR-216b expression has poorer overall survival (*P*<0.05). In our study, The results indicated that downregulated miR-216b levels were significantly associated with shorter OS time (**Figure 1D**) and the median OS time was 54.8 months. Moreover, a univariate analysis showed that differentiation, lymph node metastasis, TNM stage and miR-216b were significantly associated with OS in CRC patients (**Table 2**). A multivariate analysis also showed that miR-216b was an independent prognostic indicator for OS (**Table 2**).

miR-216b suppresses growth, migratory and invasive activity of CRC cells

To further study the regulatory role of miR-216b in CRC, HCT116 and HT29 were transfected with miR-216b mimic to upregulate its expression, qRT-PCR was used to confirm the efficiency of transfection (**Figure 2A**). We found that overexpressed miR-216b reduced CRC cell proliferation (**Figure 2B**). To exam the effect of miR-216b on the metastasis of CRC cells, we upregulated miR-216b in HCT116 and HT29. Wound-healing assay showed a significantly decrease of cell migration in miR-mimic group compared with miR-NC group (**Figure 2C**). Moreover, Transwell assay showed that the number of invasive cells in the miR-mimic group was significantly reduced compared with that in the miR-NC group (**Figure 2D**).

miR-216b inhibits angiogenesis in vitro

HUVEC tube formation assays was performed to explore whether miR-216b could inhibit

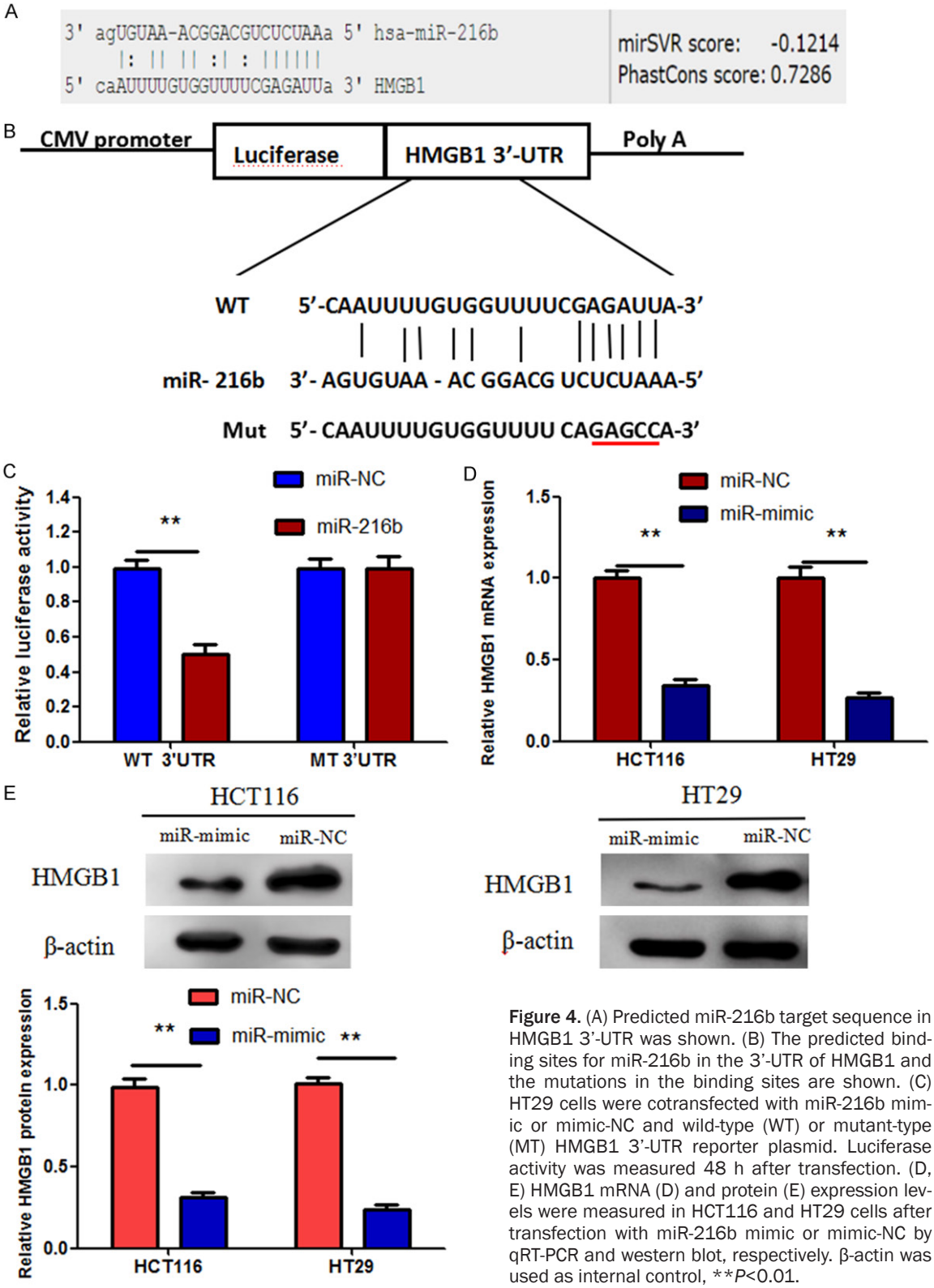

Figure 4. (A) Predicted miR-216b target sequence in HMGB1 3'-UTR was shown. (B) The predicted binding sites for miR-216b in the 3'-UTR of HMGB1 and the mutations in the binding sites are shown. (C) HT29 cells were cotransfected with miR-216b mimic or mimic-NC and wild-type (WT) or mutant-type (MT) HMGB1 3'-UTR reporter plasmid. Luciferase activity was measured 48 h after transfection. (D, E) HMGB1 mRNA (D) and protein (E) expression levels were measured in HCT116 and HT29 cells after transfection with miR-216b mimic or mimic-NC by qRT-PCR and western blot, respectively. β-actin was used as internal control, $^{**}P<0.01$.

angiogenesis in CRC. HUVECs were suspended in TCM from CRC cells and cultured wells coated by 200 μl matrigel for 6 h at 37°C. The results showed that compared with TCM from CRC cells transfected with mimic-NC, TCM from CRC cells transfected with mimic resulted in decreased tube formation of HUVECs (**Figure 2E**).

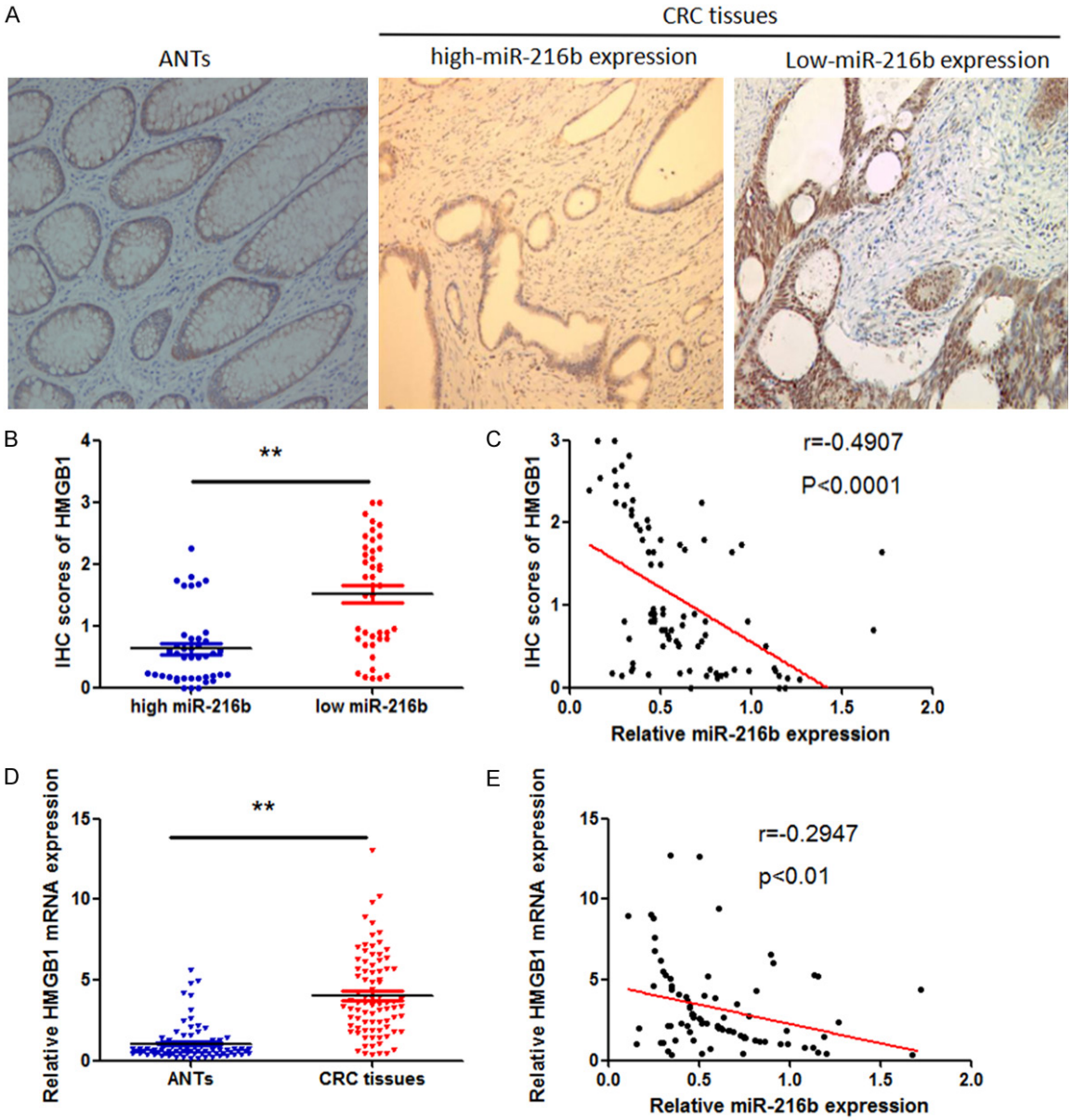

Figure 5. The relationship between miR-216b and HMGB1 in CRC tissues. A. Representative immunohistochemical staining (×200) for HMGB1 from CRC tissues and corresponding ANTs. B. IHC scores of HMGB1 in low miR-216b CRC tissues were significantly higher than that of high miR-216b CRC tissues. C. The correlation analysis were performed between the levels of miR-216b expression and ICH scores of HMGB1 in CRC tissues. D. HMGB1 mRNA in 84 CRC specimens and corresponding ANTs were assessed by qRT-PCR. E. The correlation analysis was performed between HMGB1 mRNA and miR-216b expression levels. ***P*<0.01.

The expression of HMGB1 is upregulated in CRC cell lines

To evaluate HMGB1 protein expression, western blot analysis was conducted on protein samples extracted from HCT116, HCT8, HT29 and FHC. Compared with FHC, the expression of HMGB1 protein was significantly higher in HCT116, HCT8 and HT29 (**Figure 3A**). qRT-PCR was used to determine the expression of HMGB1 mRNA in HCT116, HCT8, HT29 and FHC, we found that HCT116, HCT8 and HT29 revealed higher HMGB1 mRNA compared with those in FHC (**Figure 3B**).

HMGB1 is a direct target of miR-216b in HT29 cells

To identify the potential molecular mechanisms underlying miR-216b-induced inhibition of CRC

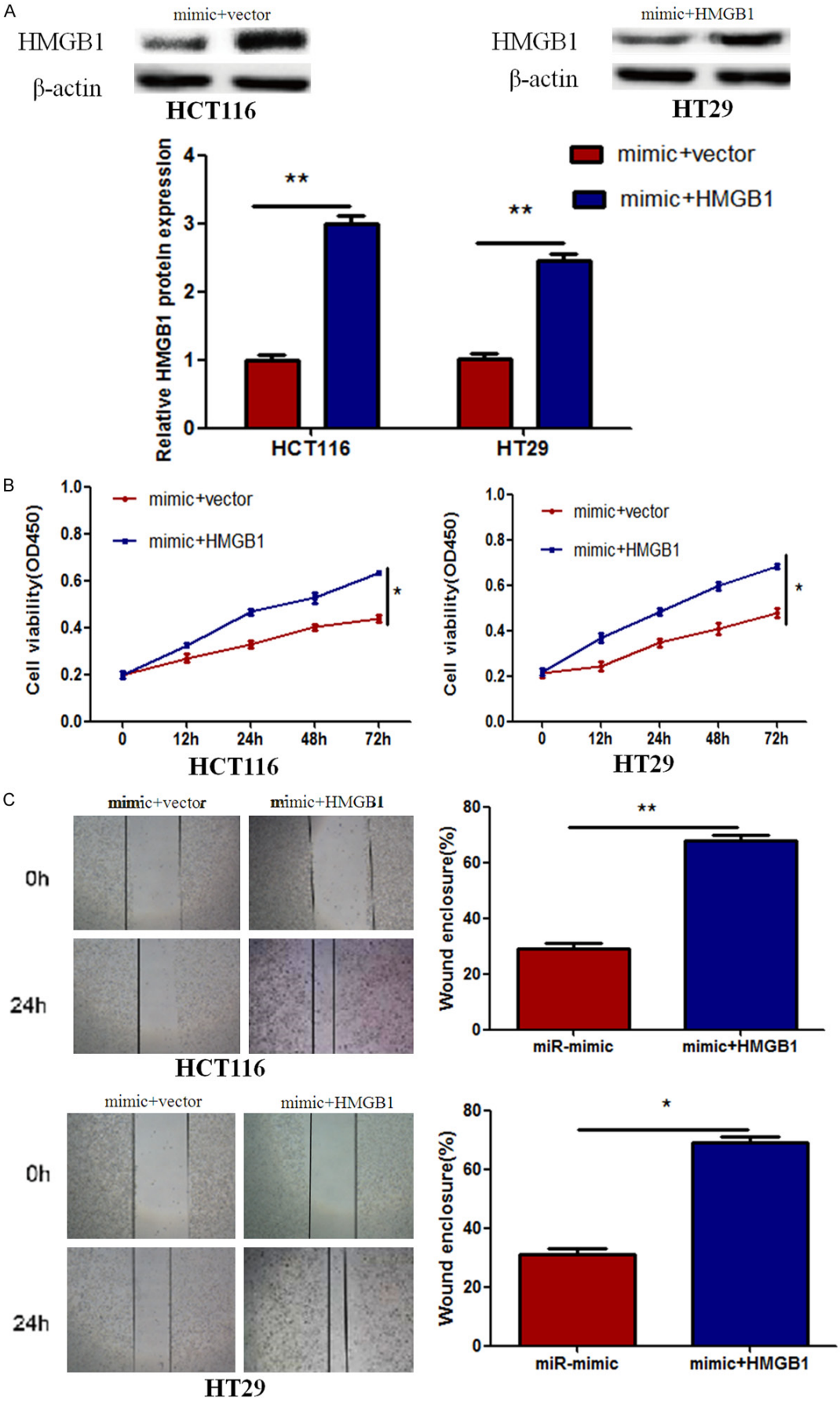
A
mimic+vector
HMGB1
β-actin
HCT116
mimic+HMGB1
HMGB1
β-actin
HT29
Relative HMGB1 protein expression
mimic+vector
mimic+HMGB1
**
**
HCT116
HT29
B
Cell viability(OD450)
mimic+vector
mimic+HMGB1
*
0
12h
24h
48h
72h
HCT116
Cell viability(OD450)
mimic+vector
mimic+HMGB1
*
HT29
C
mimic+vector
mimic+HMGB1
0h
24h
HCT116
Wound enclosure(%)
**
miR-mimic
mimic+HMGB1
mimic+vector
mimic+HMGB1
0h
24h
HT29
Wound enclosure(%)
*
miR-mimic
mimic+HMGB1

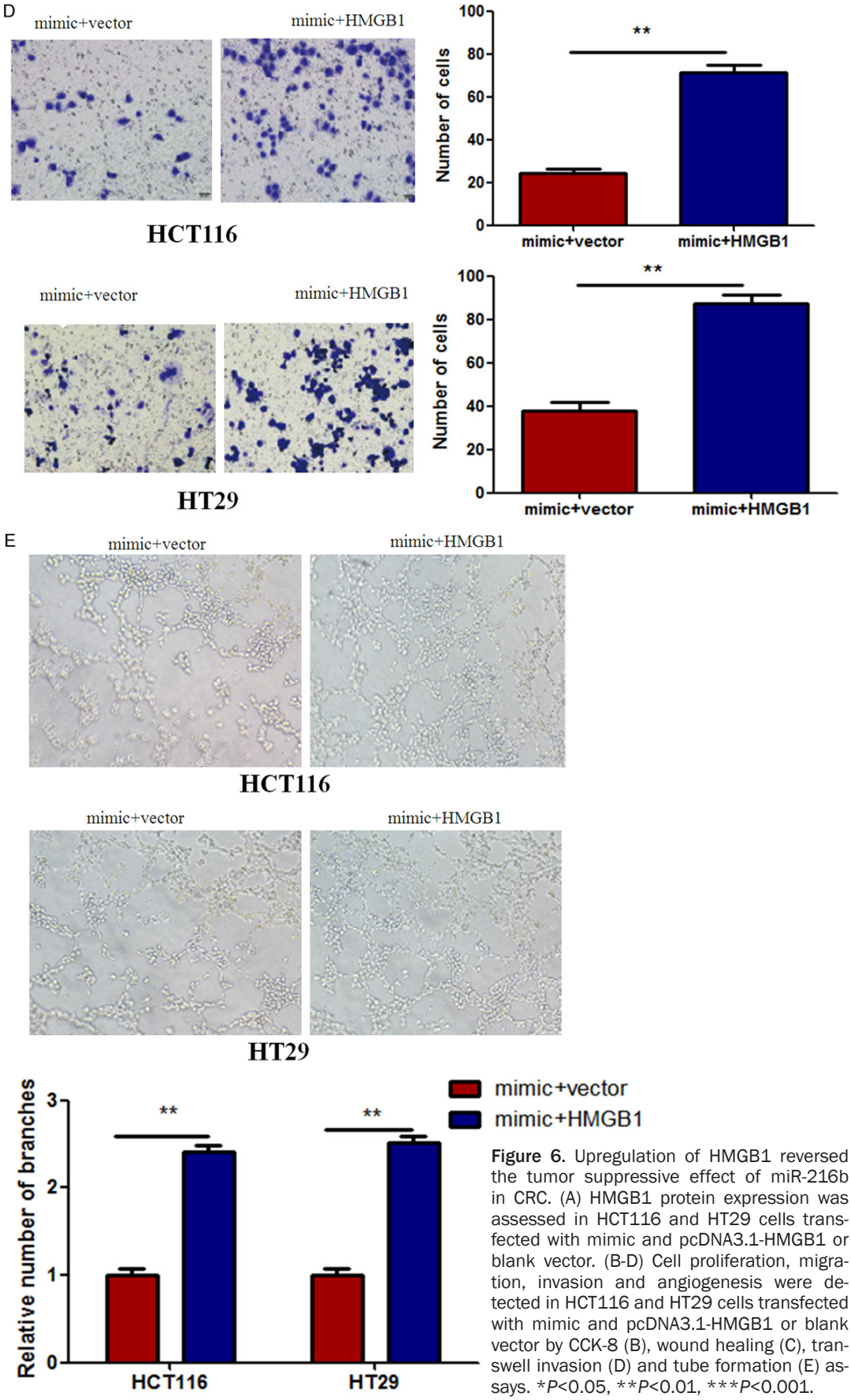

Figure 6. Upregulation of HMGB1 reversed the tumor suppressive effect of miR-216b in CRC. (A) HMGB1 protein expression was assessed in HCT116 and HT29 cells transfected with mimic and pcDNA3.1-HMGB1 or blank vector. (B-D) Cell proliferation, migration, invasion and angiogenesis were detected in HCT116 and HT29 cells transfected with mimic and pcDNA3.1-HMGB1 or blank vector by CCK-8 (B), wound healing (C), transwell invasion (D) and tube formation (E) assays. *P<0.05, **P<0.01, ***P<0.001.

biology, miRanda and Starbase were performed to analyze the potential targets of miR-216b. As shown in **Figure 4A**, HMGB1 might be a potential target gene of miR-216b, which was testified by luciferase reporter assay. The WT or MT 3'-UTR of HMGB1 was created (**Figure 4B**), each renilla luciferase vector or firefly luciferase vector was cotransfected with miR-216b mimic or mimic-NC into HT29. As shown in **Figure 4C**, the luciferase activity of HMGB1 3'-UTR-WT but not HMGB1 3'-UTR-MT was decreased approximately 50% by miR-216b mimic compared to the miR-NC, indicating that miR-216b could directly bind to the 3'-UTR of HMGB1. Subsequent experiments demonstrated that miR-216b overexpression markedly inhibited both HMGB1 mRNA and HMGB1 protein expression (**Figure 4D**, **4E**). Based on these findings, we concluded that HMGB1 is a direct target gene of miR-216b in CRC.

The relationship between miR-216b and HMGB1 in CRC tissues

To investigate whether HMGB1 up-regulation in CRC tissues compared with those in ANTs, qRT-PCR and IHC analysis were done in 84 matched CRC tissues and ANTs. protein levels of HMGB1 were found to be significantly over-expressed in CRC tissues compared with ANTs (**Figure 5A**). We also analyzed HMGB1 protein expression in CRC tissues with different miR-216b levels, the low versus high miR-216b expression was defined as the median value of miR-216b level according to the cohort of tested patients. As show in **Figure 5B**, the levels of HMGB1 protein expression in low-miR-216b CRC tissues were significantly higher than that of high-miR-216b CRC tissues, $P<0.01$. Meanwhile, a significant reverse correlation was found between HMGB1 protein levels and miR-216b expression levels in CRC tissues (**Figure 5C**). In addition, the expression of HMGB1 mRNA was also increased in CRC tissues than that in ANTs and a negative correlation was found between HMGB1 mRNA and miR-216b expression levels in CRC tissues (**Figure 5D**, **5E**).

miR-216b inhibited cell proliferation, migration, invasion and angiogenesis by targeting HMGB1

As HMGB1 has been reported to be an important oncogene in CRC [18], we speculated that HMGB1 might be involved in miR-216b-mediated inhibition of the malignant phenotypes of CRC cells. To verify our speculation, miR-216b-overexpression HCT116 and HT29 cells were further transfected with pcDNA3.1-HMGB1 plasmid to restore its expression, after transfection, western blot data showed the decreased HMGB1 level was markedly upregulated (**Figure 6A**).

CCK-8 assay, wound healing assay, transwell and tube formations assays were further used to assess the cell proliferation, migration, invasion and angiogenesis, respectively. As shown in **Figure 6B**, compared with mimic + vector group, the cell proliferation was significantly increased in the mimic + HMGB1 group. Moreover, the migratory and invasive ability of CRC cells were also higher in the mimic + HMGB1 group, when compared to those in mimic + vector group, respectively (**Figure 6C**, **6D**). Lastly, restoration of the expression of HMGB1 could also increase tube-formation ability in CRC (**Figure 6E**).

Downregulation of miR-216b activates JAK2/STAT3 signaling way through HMGB1

To investigate whether the JAK2/STAT3 signaling pathway is involved in the downregulation of miR-216b observed in HCT116 and HT29 cells, the expression levels of JAK2, p-JAK2, STAT3, p-STAT3 were measured by western blot. We found overexpression of miR-216b significantly decreased the expression of p-JAK2 and p-STAT3 protein in HCT116 and HT-29 cells (**Figure 7A**). These data showed that miR-216b upregulation might inhibit the malignant progression of CRC by inactivating the JAK2/STAT3 signaling pathway.

To further demonstrated whether miR-216b promoted the progression of CRC through HMGB1-mediated JAK2/STAT3 signaling way. HCT116 and HT29 cells were transfected with mimic along with pcDNA3.1-HMGB1 or blank vector, the results indicated that the expression of p-JAK2 and p-STAT3 were obviously increased in mimic + HMGB1 group, when compared to mimic + vector group (**Figure 7B**). Taken together, these findings implied that downregulated miR-216b activates JAK2/STAT3 signaling way through HMGB1.

miR-216b might be a potential prognostic biomarker in CRC

To determine whether plasma miR-216b could be a screening biomarker for CRC, we com-

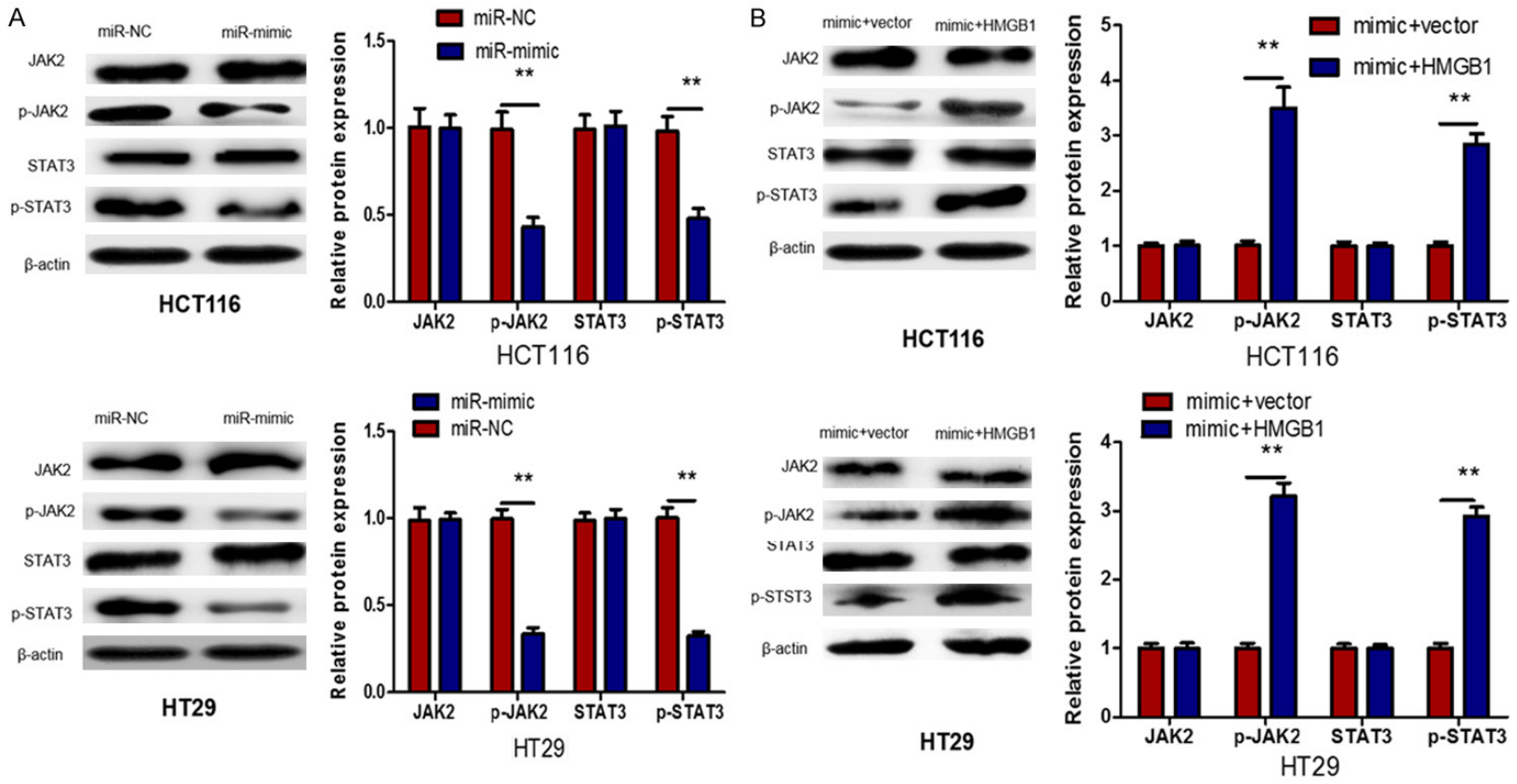

Figure 7. miR-216b promoted CRC malignant progression through JAK2/STAT3 signaling pathway. A. Representative western blotting results for JAK2, p-JAK2, STAT3 and p-STAT3 from HCT116 and HT29 cells transfected with mimic or mimic-NC, respectively. B. Representative western blotting results for JAK2, p-JAK2, STAT3 and p-STAT3 from HCT116 and HT29 cells transfected with mimic and pcDNA3.1-HMGB1 or blank vector, respectively. $^{**}P<0.01$.

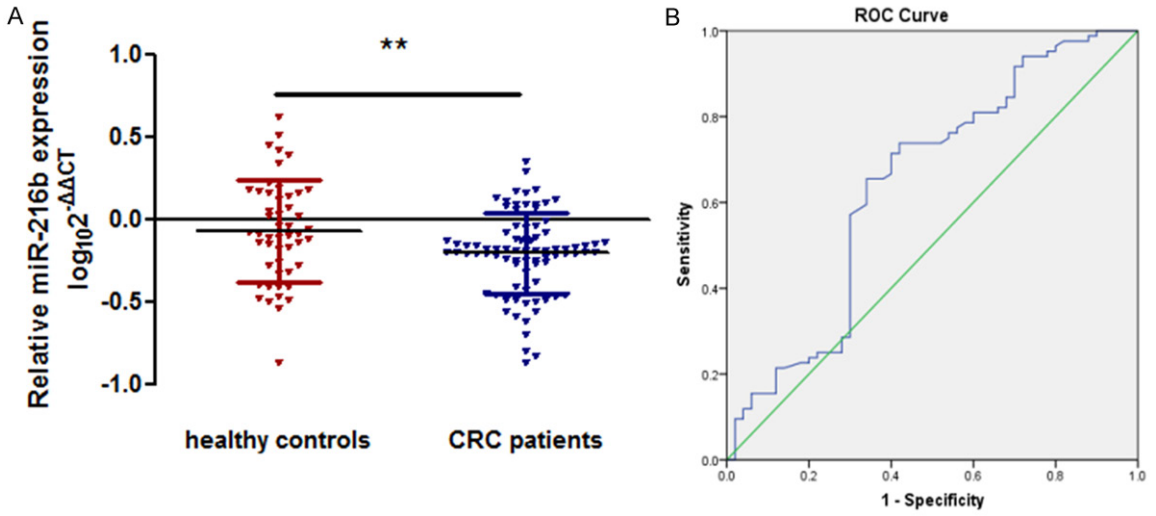

Figure 8. Plasma levels of miR-216b were downregulated in patients with CRC. A. The relative levels of miR-216b in patients with CRC and healthy controls. All data were normalized to cel-miR-39 and shown as log10. B. ROC curves for miR-216b in 84 patients with CRC and 50 healthy controls. $**P<0.01$.

pared plasma miR-216b level between healthy volunteers and patients with CRC. The results showed that plasma miR-216b level in CRC patients group was markedly lower than the levels in the healthy controls group (**Figure 8A**). An ROC curve curve was constructed for distinguishing healthy controls from CRC patients. The results indicated that the AUC was up to 0.642 (95% CI, 0.541-0.744; $p<0.1$) (**Figure 8B**). On the cutoff values from ROC curves, when the cutoff value of plasma miR-216b was -0.155, sensitivity was 66.0%, and specificity was 63.1%.

Discussion

In recent years, increasing studies have been showed that dysregulation of miRNAs, acting as tumor suppressor or oncogene, played a key role in the occurrence and development of many cancers [19-23]. Moreover, the biological functions of miRNAs in CRC are becoming recognized and increasing researches have shown dysregulated expression of miRNAs play an important role in tumorigenesis and the development of CRC [24-27].

miR-216b is a member of miR-216 family which consists of miR-216a and miR-216b, miR-216 family has been found to be altered expression in many kinds of cancers and be involved in biological process including cell proliferation, differentiation and metastasis, including pancreatic cancer [28, 29], liver cancer [11, 30], breast cancer [31], colorectal cancer [32], gastric cancer [33] and nasopharyngeal carcinoma [10]. However, the function of miR-216b in CRC is largely unknown.

In the present study, we firstly observed that miR-216b was downregulated in both human CRC tissue samples and CRC cells compared with that in ANTs or colonic mucosal epithelial cell line (FHC) by qRT-PCR. Moreover, low miR-216b was markedly associated with the TNM stage, lymph node metastases, differentiation and poor OS. Kaplan-Meier survival analysis and log-rank tests were also performed to investigate the correlation between miR-216b expression and prognosis of CRC patients, we found that patients with lower miR-216b expression had a obviously poorer prognosis than those with higher miR-216b expression. In addition, after up-regulating the expression of miR-216b by transfecting with mimic in HCT-116 and HT-29 cells, we found overexpression of miR-216b could not only inhibit CRC cell proliferation by CCK-8 assay, but reduce the migratory and invasive ability of CRC cells using wound-healing assay and transwell assay. Lastly, our results verified that upregulation miR-216b could suppress angiogenesis by tube formation assay.

HMGB1, normally located in the nucleus, can be released by tumor cells and inflammatory

cells [34]. Recently, increasing studies have demonstrated that HMGB1 expression in CRC tissues was significantly up-regulated compared with that in corresponding non-cancerous mucosa [35], which was consistent with our data. In addition, overexpression of HMGB1 has also been correlated with invasion, metastasis and poor prognosis in CRC [18]. These studies suggested that HMGB1 functioned as an oncogene in CRC.

It is well known that miRNAs perform their function by regulating their target genes. HMGB1 has been reported to a target gene of many miRNAs, including miR320a [36], miR-193a-3p [37], miR-142 [38] and miR-218 [39]. Here, bioinformatics analysis indicated HMGB1 might be the functional target gene for miR-216b. Next, a luciferase reporter assay was performed to demonstrate that HMGB1 is a direct target of miR-216b as showed that ectopic expression of miR-216b decreased luciferase activity of the WT HMGB1-3'UTR and miR-216b downregulated HMGB1 expression both on mRNA and protein level. What's more, we found that HMGB1 mRNA and protein expression in CRC was obviously increased compared with that in FHC or ANTs, which was inversely correlated with miR-216b in CRC tissues. Besides, we also verified that HMGB1 upregulation could reverse the effects on cell proliferation, migration and invasion mediated by miR-216b overexpression in CRC cells. Furthermore, increasing studies have reported that HMGB1 could contribute tumor angiogenesis in various cancers, including colorectal cancer [40, 41], and our results showed miR-216b in CRC involved in regulation of HUVECs angiogenesis at least partially depended on the regulation of HMGB1. These results indicated that miR-216b functioned as a tumor suppressor by inhibiting HMGB1 expression.

Previous research showed that HMGB1 was engaged in JAK/STAT/NF-κB signaling pathway [42-44], and JAK2/STAT3/NF-κB signaling are critical for the progression and development of various cancers, making them focal points of cancer research [45-49]. In this study, we found that p-JAK2 and p-STAT3 protein levels were decreased by miR-216b overexpression. To further explore the mechanism that might be involved in the miR-216b associated malignant progression of CRC, we examined the effect of miR-216b-mediated HMGB1 regulation on JAK2/STAT3 activation. Our study showed that the expression of p-JAK2 and p-STAT3 were markedly upregulated in mimic + HMGB1 group, when compared to mimic + vector group. These results indicated that downregulated miR-216b promoted the development and progression of CRC, at least partially by targeting HMGB1-mediated JAK2/STAT3 pathway.

Lastly, we tested the diagnostic value of plasma miR-216b in differentiating people without CRC from CRC patients. We observed that plasma miR-216b levels from CRC patients were significantly lower than the levels from healthy controls. This result suggested that plasma miR-216b had a potential diagnostic value in CRC.

Conclusion

In summary, our study showed that miR-216b was downregulated in CRC tissue samples and cell lines. Moreover, the expression of miR-216b was reversely associated with the TNM stage, lymph node metastases, differentiation and poor OS. Mechanistically, we demonstrated that miR-216b inhibited proliferation, migration, invasion and angiogenesis of CRC by targeting HMGB1. Additionally, we showed that downregulated miR-216b might promote the development and progression of CRC at least partially through JAK2/STAT3 signaling way. Lastly, we found the expression of plasma miR-216b was decreased in CRC patients compared with that in healthy controls. These findings may provide a new insight into the molecular mechanism of CRC, and implied that miR-216b might be a potential biomarker and therapeutic target for CRC.

Acknowledgements

This project was supported by grants from the National Nature Science Foundation of China (No. 81472027, 81501820) to SKW and YQP; Innovation team of Jiangsu provincial health-strengthening engineering by science and education to SKW.

Abbreviations

CRC, colorectal cancer; HMGB1, High mobility group box 1; qRT-PCR, quantitative real-time PCR; JAK2, Janus kinase 2; STAT3, signal transducer and activator of transcription 3; IHC,

immunohistochemistry; CCK-8, Cell Counting Kit-8; ANTs, adjacent normal tissues; OS, overall survival; MiRs, MicroRNAs; 3'-UTRs, 3'-untranslated regions; NPC, nasopharyngeal carcinoma; DMEM, Dulbecco's modified Eagle medium; FBS, fetal bovine serum; NC, negative control; ECL, enhanced chemiluminescence system; ROC, receiver operating characteristic.

Address correspondence to: Shukui Wang, Medical college, Southeast University, Nanjing 210009, Jiangsu, China; General Clinical Research Center, Nanjing First Hospital, Nanjing Medical University, Nanjing 210006, Jiangsu, China. E-mail: sk_wang@njmu.edu.cn

References

[1] Siegel RL, Miller KD and Jemal A. Cancer statistics, 2017. CA Cancer J Clin 2017; 67: 7-30.
[2] Brody H. Colorectal cancer. Nature 2015; 521: S1.
[3] Peters U, Bien S and Zubair N. Genetic architecture of colorectal cancer. Gut 2015; 64: 1623-1636.
[4] Chen Q, Li Y, Li Z, Zhao Q and Fan L. Overexpression of PTP1B in human colorectal cancer and its association with tumor progression and prognosis. J Mol Histol 2014; 45: 153-159.
[5] Choi E, Choi E and Hwang KC. MicroRNAs as novel regulators of stem cell fate. World J Stem Cells 2013; 5: 172-187.
[6] Ambros V. The functions of animal microRNAs. Nature 2004; 431: 350-355.
[7] Bartel DP. MicroRNAs: genomics, biogenesis, mechanism, and function. Cell 2004; 116: 281-297.
[8] Di Leva G and Croce CM. miRNA profiling of cancer. Curr Opin Genet Dev 2013; 23: 3-11.
[9] Grady WM and Tewari M. The next thing in prognostic molecular markers: microRNA signatures of cancer. Gut 2010; 59: 706-708.
[10] Deng M, Tang H, Zhou Y, Zhou M, Xiong W, Zheng Y, Ye Q, Zeng X, Liao Q, Guo X, Li X, Ma J and Li G. miR-216b suppresses tumor growth and invasion by targeting KRAS in nasopharyngeal carcinoma. J Cell Sci 2011; 124: 2997-3005.
[11] Wang F, Ying HQ, He BS, Pan YQ, Deng QW, Sun HL, Chen J, Liu X and Wang SK. Upregulated lncRNA-UCA1 contributes to progression of hepatocellular carcinoma through inhibition of miR-216b and activation of FGFR1/ERK signaling pathway. Oncotarget 2015; 6: 7899-7917.
[12] Bianchi ME and Manfredi AA. High-mobility group box 1 (HMGB1) protein at the crossroads between innate and adaptive immunity. Immunol Rev 2007; 220: 35-46.
[13] Muller S, Scaffidi P, Degryse B, Bonaldi T, Ronfani L, Agresti A, Beltrame M and Bianchi ME. New EMBO members' review: the double life of HMGB1 chromatin protein: architectural factor and extracellular signal. EMBO J 2001; 20: 4337-4340.
[14] Moriwaka Y, Luo Y, Ohmori H, Fujii K, Tatsumoto N, Sasahira T and Kuniyasu H. HMGB1 attenuates anti-metastatic defense of the lymph nodes in colorectal cancer. Pathobiology 2010; 77: 17-23.
[15] Stoetzer OJ, Fersching DM, Salat C, Steinkohl O, Gabka CJ, Hamann U, Braun M, Feller AM, Heinemann V, Siegele B, Nagel D and Holdenrieder S. Circulating immunogenic cell death biomarkers HMGB1 and RAGE in breast cancer patients during neoadjuvant chemotherapy. Tumour Biol 2013; 34: 81-90.
[16] Liu PL, Tsai JR, Hwang JJ, Chou SH, Cheng YJ, Lin FY, Chen YL, Hung CY, Chen WC, Chen YH and Chong IW. High-mobility group box 1-mediated matrix metalloproteinase-9 expression in non-small cell lung cancer contributes to tumor cell invasiveness. Am J Respir Cell Mol Biol 2010; 43: 530-538.
[17] Song B, Song WG, Li ZJ, Xu ZF, Wang XW, Wang CX and Liu J. Effect of HMGB1 silencing on cell proliferation, invasion and apoptosis of MGC-803 gastric cancer cells. Cell Biochem Funct 2012; 30: 11-17.
[18] Yao X, Zhao G, Yang H, Hong X, Bie L and Liu G. Overexpression of high-mobility group box 1 correlates with tumor progression and poor prognosis in human colorectal carcinoma. J Cancer Res Clin Oncol 2010; 136: 677-684.
[19] Liu Y, Liu R, Yang F, Cheng R, Chen X, Cui S, Gu Y, Sun W, You C, Liu Z, Sun F, Wang Y, Fu Z, Ye C, Zhang C, Li J and Chen X. miR-19a promotes colorectal cancer proliferation and migration by targeting TIA1. Mol Cancer 2017; 16: 53.
[20] Liu L, Bi N, Wu L, Ding X, Men Y, Zhou W, Li L, Zhang W, Shi S, Song Y and Wang L. MicroRNA-29c functions as a tumor suppressor by targeting VEGFA in lung adenocarcinoma. Mol Cancer 2017; 16: 50.
[21] Teng Y, Ren Y, Hu X, Mu J, Samykutty A, Zhuang X, Deng Z, Kumar A, Zhang L, Merchant ML, Yan J, Miller DM and Zhang HG. MVP-mediated exosomal sorting of miR-193a promotes colon cancer progression. Nat Commun 2017; 8: 14448.
[22] Li P, Yang Y, Liu H, Yang AK, Di JM, Tan GM, Wang HF, Qiu JG, Zhang WJ, Jiang QW, Zheng DW, Chen Y, Wei MN, Huang JR, Wang K, Shi Z and Ye J. MiR-194 functions as a tumor suppressor in laryngeal squamous cell carcinoma by targeting Wee1. J Hematol Oncol 2017; 10: 32.

[23] Liu C, Liu R, Zhang D, Deng Q, Liu B, Chao HP, Rycaj K, Takata Y, Lin K, Lu Y, Zhong Y, Krolewski J, Shen J and Tang DG. MicroRNA-141 suppresses prostate cancer stem cells and metastasis by targeting a cohort of pro-metastasis genes. Nat Commun 2017; 8: 14270.
[24] Zhao S, Sun H, Jiang W, Mi Y, Zhang D, Wen Y, Cheng D, Tang H, Wu S, Yu Y, Liu X, Cui W, Zhang M, Sun X, Zhou Z, Peng Z and Yan D. miR-4775 promotes colorectal cancer invasion and metastasis via the Smad7/TGFbeta-mediated epithelial to mesenchymal transition. Mol Cancer 2017; 16: 12.
[25] Lu D, Yao Q, Zhan C, Le-Meng Z, Liu H, Cai Y, Tu C, Li X, Zou Y and Zhang S. MicroRNA-146a promote cell migration and invasion in human colorectal cancer via carboxypeptidase M/src-FAK pathway. Oncotarget 2017; 8: 22674-22684.
[26] Matsuyama R, Okuzaki D, Okada M and Oneyama C. MicroRNA-27b suppresses tumor progression by regulating ARFGEF1 and focal adhesion signaling. Cancer Sci 2016; 107: 28-35.
[27] Li Y, Kuscu C, Banach A, Zhang Q, Pulkoski-Gross A, Kim D, Liu J, Roth E, Li E, Shroyer KR, Denoya PI, Zhu X, Chen L and Cao J. miR-181a-5p inhibits cancer cell migration and angiogenesis via downregulation of matrix metalloproteinase-14. Cancer Res 2015; 75: 2674-2685.
[28] Bofill-De RX, Gironella M and Fillat C. miR-148a- and miR-216a-regulated oncolytic adenoviruses targeting pancreatic tumors attenuate tissue damage without perturbation of miRNA activity. Mol Ther 2014; 22: 1665-1677.
[29] Hou BH, Jian ZX, Cui P, Li SJ, Tian RQ and Ou JR. miR-216a may inhibit pancreatic tumor growth by targeting JAK2. Febs Lett 2015; 589: 2224-2232.
[30] Chen PJ, Yeh SH, Liu WH, Lin CC, Huang HC, Chen CL, Chen DS and Chen PJ. Androgen pathway stimulates microRNA-216a transcription to suppress the tumor suppressor in lung cancer-1 gene in early hepatocarcinogenesis. Hepatology 2012; 56: 632-643.
[31] Jeyapalan Z, Deng Z, Shatseva T, Fang L, He C and Yang BB. Expression of CD44 3'-untranslated region regulates endogenous microRNA functions in tumorigenesis and angiogenesis. Nucleic Acids Res 2011; 39: 3026-3041.
[32] Zhang D, Zhao L, Shen Q, Lv Q, Jin M, Ma H, Nie X, Zheng X, Huang S, Zhou P, Wu G and Zhang T. Down-regulation of KIAA1199/CEMIP by miR-216a suppresses tumor invasion and metastasis in colorectal cancer. Int J Cancer 2017; 140: 2298-2309.
[33] Wang Y, Xu P, Yao J, Yang R, Shi Z, Zhu X, Feng X and Gao S. MicroRNA-216b is down-regulated in human gastric adenocarcinoma and inhibits proliferation and cell cycle progression by targeting oncogene HDAC8. Target Oncol 2016; 11: 197-207.
[34] Yang H, Rivera Z, Jube S, Nasu M, Bertino P, Goparaju C, Franzoso G, Lotze MT, Krausz T, Pass HI, Bianchi ME and Carbone M. Programmed necrosis induced by asbestos in human mesothelial cells causes high-mobility group box 1 protein release and resultant inflammation. Proc Natl Acad Sci U S A 2010;107: 12611-12616.
[35] Volp K, Brezniceanu ML, Bosser S, Brabletz T, Kirchner T, Gottel D, Joos S and Zornig M Increased expression of high mobility group box 1 (HMGB1) is associated with an elevated level of the antiapoptotic c-IAP2 protein in human colon carcinomas. Gut 2006; 55: 234-242.
[36] Lv G, Wu M, Wang M, Jiang X, Du J, Zhang K, Li D, Ma N, Peng Y, Wang L, Zhou L, Zhao W, Jiao Y, Gao X and Hu Z. miR-320a regulates high mobility group box 1 expression and inhibits invasion and metastasis in hepatocellular carcinoma. Liver Int 2017; 37: 1354-1364.
[37] Khoo CP, Roubelakis MG, Schrader JB, Tsaknakis G, Konietzny R, Kessler B, Harris AL and Watt SM. miR-193a-3p interaction with HMGB1 downregulates human endothelial cell proliferation and migration. Sci Rep 2017; 7: 44137.
[38] Jiang D, Wang H, Li Z, Li Z, Chen X and Cai H. MiR-142 inhibits the development of cervical cancer by targeting HMGB1. Oncotarget 2017; 8: 4001-4007.
[39] Gu J, Xu R, Li Y, Zhang J and Wang S. MicroRNA-218 modulates activities of glioma cells by targeting HMGB1. Am J Transl Res 2016; 8: 3780-3790.
[40] Chung HW and Lim JB. High-mobility group box-1 contributes tumor angiogenesis under interleukin-8 mediation during gastric cancer progression. Cancer Sci 2017; 108: 1594-1601.
[41] Zhu L, Ren L, Chen Y, Fang J, Ge Z and Li X. Redox status of high-mobility group box 1 performs a dual role in angiogenesis of colorectal carcinoma. J Cell Mol Med 2015; 19: 2128-2135.
[42] Tang D, Kang R, Zeh HR and Lotze MT. High-mobility group box 1 and cancer. Biochim Biophys Acta 2010;1799: 131-140.
[43] Lu B, Antoine DJ, Kwan K, Lundback P, Wahamaa H, Schierbeck H, Robinson M, Van Zoelen MA, Yang H, Li J, Erlandsson-Harris H, Chavan SS, Wang H, Andersson U and Tracey KJ. JAK/STAT1 signaling promotes HMGB1 hyperacetylation and nuclear translocation. Proc Natl Acad Sci U S A 2014; 111: 3068-3073.
[44] Li Y, He J, Zhong D, Li J and Liang H. High-mobility group box 1 protein activating nuclear

factor-kappaB to upregulate vascular endothelial growth factor C is involved in lymphangiogenesis and lymphatic node metastasis in colon cancer. J Int Med Res 2015; 43: 494-505.

[45] Kim B, Kim HS, Kim S, Haegeman G, Tsang BK, Dhanasekaran DN and Song YS. Adipose stromal cells from visceral and subcutaneous fat facilitate migration of ovarian cancer cells via IL-6/JAK2/STAT3 pathway. Cancer Res Treat 2017; 49: 338-349.

[46] Wormann SM, Song L, Ai J, Diakopoulos KN, Kurkowski MU, Gorgulu K, Ruess D, Campbell A, Doglioni C, Jodrell D, Neesse A, Demir IE, Karpathaki AP, Barenboim M, Hagemann T, Rose-John S, Sansom O, Schmid RM, Protti MP, Lesina M and Algul H. Loss of P53 function activates JAK2-STAT3 signaling to promote pancreatic tumor growth, stroma modification, and gemcitabine resistance in mice and is associated with patient survival. Gastroenterology 2016; 151: 180-193.

[47] Gasparini C, Celeghini C, Monasta L and Zauli G. NF-κB pathways in hematological malignancies. Cell Mol Life Sci 2014; 71: 2083-2102.

[48] Sokolova O and Naumann M. NF-kappaB signaling in gastric cancer. Toxins (Basel) 2017; 9.

[49] Nagaraju GP, Mezina A, Shaib WL, Landry J and El-Rayes BF. Targeting the Janus-activated kinase-2-STAT3 signalling pathway in pancreatic cancer using the HSP90 inhibitor ganetespib. Eur J Cancer 2016; 52: 109-119.